IJHSR
ijhighschoolresearch.org
RESEARCH ARTICLE

Sun-Aware Routing for Enhanced Driving Safety Using A* Search and Real-Time Atmospheric Conditions

Rohin Vig

Mission San Jose High School, 41717 Palm Avenue, Fremont, California, 94539, USA; vohinr@icloud.com

ABSTRACT: Sun glare is one of the most common natural causes of traffic accidents and can also contribute to the disengagement of camera-based autonomous vehicles, leading to uncomfortable or unsafe transitions back to human control. Traditional navigation systems ignore the position of the sun, which can significantly reduce visibility and safety during commutes, especially during sunrise and sunset. This paper presents a routing algorithm for minimizing sun glare exposure in navigation during sunset commutes. It uses solar position data from PySolar and road networks in the form of NetworkX graphs from OpenStreetMap (OSM) to compute sun-aware routes using the A* search algorithm. The cost function assigned to each edge in the NetworkX road graph is a linear combination of the sun position and travel time. Unlike prior methods, it integrates real-time cloud cover data and evaluates disengagement reduction for paths evaluated using this sun-aware routing algorithm. It achieves up to a median 36% decrease in aggregate glare as measured by a cost function which uses sun position as a proxy for glare while keeping the travel time to within a median 15.4% increase of the benchmark. When applied to real-world disengagement data from a 2021 Tesla Model Y, the algorithm demonstrates preliminary evidence of a statistically significant reduction in autopilot disengagements in a small, single-vehicle trial under clear-sky conditions during sunset, with up to a median 33.3% fewer high-glare segments while keeping the travel time to within a median 14.6% increase of the benchmark. This proposed algorithm was tested using NetworkX shortest_path paths as a benchmark. Future extensions of this project could include developing a more generalized routing graph with time-varying penalties incorporating dynamic factors like real-time traffic and weather conditions, and roadside obstacle-aware glare modeling for more accurate navigation.

KEYWORDS: Systems Software, Algorithms, A* Routine Algorithm, Dynamic Routing.

Introduction

Thousands of crashes happen every year because drivers are blinded by the sun, and current GPS systems don't address this problem. Commonly used navigation systems like Google Maps, Apple Maps, or Waze do not take temporally-dependent environmental factors into account while calculating routes, opting to optimise for either distance or time. Sun glare was the second most common factor in approximately 9,000 car crashes, second only to slick roads, representing about 17% of the 52,000 crashes with environmental-related critical reasons surveyed by the National Motor Vehicle Crash Causation Survey (NMVCCS), where Emergency Medical Services were dispatched.[1]

While least-time or least-distance courses may be an optimal approach during times when the sun does not interfere with vision, such routes might cause accidents on affected roads. Bahnesen and Mayster show that driving with sun glare can result in (i) visual impairment, (ii) delayed reaction time, (iii) increased risk of accidents, and (iv) driver distraction and discomfort.[2] Das *et al.* list seven key factors that influence glare risk, (i) relative sun position, (ii) cloud cover, (iii) atmospheric refraction, (iv) heights of buildings and trees along the road(s) traveled, (v) road infrastructure like tunnels and overpasses, (vi) reflectivity of the surrounding buildings and objects, and (vii) reflectivity of the road's surface.[3]

To quantify glare more specifically, Guo *et al.* measured the relative position of the sun as measured by the azimuthal and altitudinal angles from the driver's eyes, which resulted in the most glare being an azimuthal angle between (-57.7°, 57.7°) and an altitudinal angle (5.6°, 29.0°).[4] In this case, the azimuthal angle is defined as the angle between the driving direction and solar azimuth, not relative to true north. By integrating sun position and vehicle-specific glare sensitivity into navigation, we can improve driver safety without significantly compromising travel-time.

Previous work has explored partial solutions to glare-aware navigation. Das *et al.* introduced a dynamic glare-aware routing approach based on sun angle data.[3] Li *et al.* proposed a method to detect obstacles like trees and buildings blocking sunlight in cities using Google Street View (GSV) to create an obstacle-aware glare model for more accurate navigation.[5] However, these models do not incorporate real-time atmospheric conditions. To address this gap, we extend prior work by integrating live cloud cover data from Open-Meteo and weighting schemes based on user feedback into a dynamic sun-aware routing algorithm.

Our sun-aware routing algorithm is compared to a shortest path route generated using the nx.shortest_path function as a benchmark for statistical analysis. A route will be modified from its time or distance optimized counterpart when it directs the commuter to proceed directly towards either a sunrise or a sunset. However, this may result in dramatically higher travel times and distances. We evaluate how much a sun-aware routing algorithm can reduce sun glare exposure during sunset

DOI: 10.36838/IJHSR87.308

commutes by comparing its performance against the fastest route provided by Google Maps using a glare metric based on solar position along the path. We further evaluate the effectiveness of our algorithm by measuring the difference in the number of disengagements a Tesla Model Y experiences while travelling a solar-optimized route versus a shortest path route given by the NetworkX module. We used the shortest path route from NetworkX because, unlike other routes from services like Google Maps, it doesn't account for live traffic conditions.

Methods

This routing algorithm modifies traditional A* search to account for sun glare during travel. The system integrates real-world geographic data, solar position calculations, and real-time weather data to generate routes that effectively minimise both travel time and glare exposure. The overall pipeline consists of four key components: graph construction, sun glare modeling, cost function design and weight assignment, and customized A* search.

Graph Construction:

We begin by generating a Directed Multidigraph from real-world geographical road network data from OpenStreetMap's Python module OSMnx. Each node in the graph represents an intersection. We filter out nodes with fewer than 3 roads intersecting there. This means dead ends and cul-de-sacs are removed - only four-way and T-intersections are considered in the map. Furthermore, we filter out undrivable roads. Then, we convert the data from the ECEF (Earth Center, Earth Fixed) coordinates provided by OpenStreetMap to Latitude and Longitude for the convenience of subsequent steps. Using this location data, a sun-glare weight can be calculated and assigned to the edges between two nodes.

Sun Glare Modeling:

In order to quantify the amount of glare entering a driver's eyes, we use a custom cost function by using the position of the sun as a proxy for sun glare. We use the Python module *PySolar* to get accurate solar position relative to a point on the Earth's surface at any time, given the azimuthal angle θ and the altitudinal angle ϕ. From here on, the azimuthal angle refers to the angle measured relative to true north. Note that the numbers *PySolar* produces are a result of mathematical computation and modeling of solar position instead of real-time experimental values.

To be useful as a sun glare penalty, this cost function must have two characteristics:

1) It must be large when the sun is closer to the horizon and small when it is near midday or under the horizon.

2) It must be large when the driver is facing toward the sun and small when the driver is facing away.

To address the first characteristic, the cost function must have a factor of $1-\sin(\theta)$ This function has a maximum when ϕ=0 and a minimum when θ=90°. However, to address the glare penalty going to zero when the sun is under the horizon, we must take the maximum of $1-\sin(\theta)$ with 0. Therefore, the first factor of the glare penalty function is $glarePenalty = max(0,1 - sin(\theta))$.

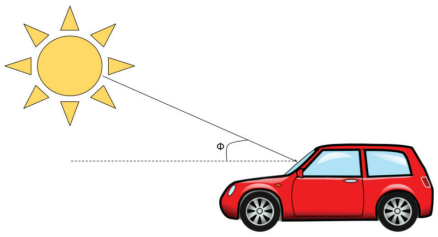

Figure 1: This figure depicts the definition of the altitude of the sun and shows that a higher weight should be assigned to smaller values of ϕ.

Furthermore, one can intuitively see from Figure 1 that a driver would have less glare if they are heading in a direction that is not pointed straight at a sunrise or sunset. Hence, we multiply again by the cosine of the difference between the sun's azimuth with respect to north and the car's heading with respect to north to fulfill the second characteristic, $cos(|\ \varphi - \phi\ |)$. To prevent the azimuthal component of this glare penalty function from going below zero, we take the maximum between it and 0, $max(0, cos(|\ \varphi - \phi\ |))$.

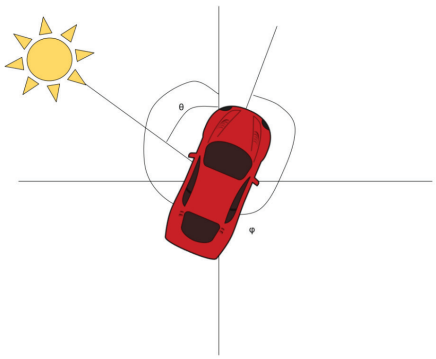

Figure 2: This figure depicts the definition of the relative azimuth of the sun as $|\ \varphi - \phi\ |$ and shows that if $|\ \varphi - \phi\ |$ were greater than 90°, the car would be facing away from the sun. Hence, routes facing away from the sun experience minimal glare, guiding the algorithm to favor such headings.

$$GlarePenalty = max(0,1 - sin(\theta)) \cdot max(0, cos(|\ \varphi - \phi\ |)) \quad (1)$$

If the altitude is less than zero, the sun is under the horizon, and the cost function is assigned the value 0. Similarly, from Figure 2, if the car is facing more than 90° away from the sun in either direction, the sun is behind the driver, and the cost function is assigned the value 0. The final pseudocode for the solar component of the cost function is as follows:

```
Function SolarCost(latitude, longitude, azimuth_facing, date):
  If date is not given:
    Set date to default datetime (2025-05-12 19:30:00 UTC)

  altitude ← get sun altitude at (latitude, longitude, date)
  azimuth  ← get sun azimuth at (latitude, longitude, date)

  If altitude ≤ 0:
    Return 0

  angle_diff ← absolute angular difference between azimuth and
azimuth_facing
  cos_diff   ← cos(angle_diff in radians)
  sin_alt    ← sin(altitude in radians)

  glare_cost ← (1 - sin_alt) × max(0, cos_diff)

  Return glare_cost
```

In order to calculate the glare component of the edge cost function, we sample multiple evenly spaced points between two nodes and take the average glare value across those points. While this approach is effective for relatively straight roads, it could lead to incorrect modelling for curvy roads. We don't address this limitation in this paper beyond this short disclaimer and leave a more thorough treatment of this issue to future research.

Figure 3 shows the value of the cost function at different times throughout the day. As per intuition, the figure shows spikes during sunrise and sunset when the glare is the highest, and smaller values as midday approaches and during the night.

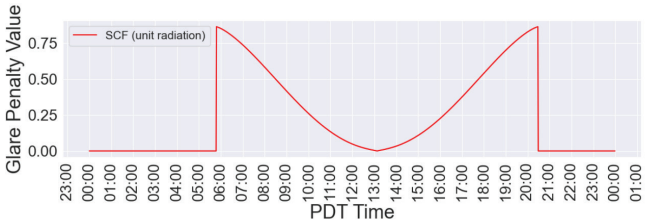

Figure 3: This figure shows the values of the glare cost function evaluated at 37.5, -122 latitude and longitude on June 12, 2025. This is taken as the aggregate of a measurement taken facing east and west. The sun rose at 5:46 AM PDT and set at 8:30 PM PDT. The glare peaks at sunrise and sunset, validating the efficacy of this cost function.

Edge Cost Function:

We define a custom edge cost function as a weighted sum of travel time on that edge and glare penalty:

$$cost(e) = \alpha \cdot glarePenalty\,(e) \cdot (1\text{-}\alpha) \cdot travelTimePenalty(e) \qquad (2)$$

To ensure the two components are comparable and that the weights α are more interpretable, both the distance and glare penalty terms are normalized across the entire graph using min-max normalisation:

$$X_{norm} = \frac{X - min(X)}{max(X) - min(X)} \qquad (3)$$

This normalisation allows for consistent scaling throughout the graph, allowing the cost function to reflect the desired trade-off between distance and glare-avoidance.

Additionally, before being added to the travel time component of the cost function, the glare penalty is multiplied by a coefficient representing cloud conditions. When queried for cloud cover data, *Open-Meteo* outputs a number between 0 and 1 representing what percent of the sky is covered with clouds at a given location. The cloud conditions multiplier is simply 1-γ where γ is the percent of the sky covered with clouds.

$$cost(e) = (1\text{-}\gamma) \cdot \alpha \cdot glarePenalty(e) + (1\text{-}\alpha) \cdot travelTimePenalty(e) \qquad (4)$$

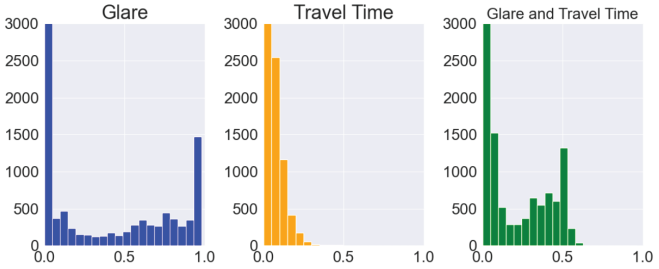

Figure 4: This figure shows the frequency of each value of the glare and travel time components of the cost function for Fremont, California, at 8:00 PM on June 15, 2025. The glare component has not been multiplied by the cloud conditions multiplier. The travel time weights are heavily skewed to the right, while the glare component is more uniformly distributed. This means that the α-value does not effectively represent the relative importance of glare and travel time in this cost function. However, this is not particularly relevant to our analysis since it relies on comparing these α-values.

Note in Figure 4, most of the values are centered around 0. For the glare cost, this is because half of the roads in the graph face away from the sun, therefore earning a glare cost close to 0. Simultaneously, the cars travelling on the other lane of the two-way road face directly toward the sun. These roads are the ones responsible for the cluster around 0.8. The graph of travel time looks highly skewed to the right because most roads in the city of Fremont are residential streets and intersect abundantly with each other. Since each intersection is a node in the graph, many edges have a small travel time weight associated with them.

The tunable parameters α were chosen by looping through values of α between 0 and 1 in increments of 0.1 and determining whether the difference in travel times and aggregate glare between the benchmark paths and custom paths sampled across 500 points is statistically significant for that coefficient. The benchmark paths of this statistical analysis were simply the shortest path between two nodes.

The primary objective of this analysis was to determine the statistical significance of the observed differences in two key areas: travel times and aggregate glare. We did this using the Wilcoxon signed-rank test since the results of a Shapiro-Wilk test on the distributions of percentage improvement in aggregate glare, number of disengagements, and travel times were statistically significant. These differences were evaluated by comparing the performance of benchmark paths against a set of custom paths from our sun-aware routing algorithm, evaluated on 500 distinct westward start-end pairs to ensure a representative dataset. The statistical significance testing aimed to determine whether the observed variations were genuine and attributable to the parameter adjustments, rather than merely random fluctuations.

This exploration allowed for a detailed understanding of how changes in the tunable parameters influenced the overall system performance, as well as helped us determine which parameter resulted in the best improvement in aggregate glare while keeping the sun-aware path's travel time to within a 20% increase of the benchmark travel time. A 20% increase in travel time was chosen as a practical threshold to balance improved glare reduction with acceptable delays for typical drivers.

DOI: 10.36838/IJHSR87.308

A Search Algorithm:*

We apply the A* algorithm to compute the shortest path with respect to our custom cost function. A crucial part of the A* algorithm is the heuristic, which is an optimistic estimate (underestimate) of the distance between every node and the destination node. The heuristic used is the great-circle distance (Haversine Distance) between the current node and the destination. This is an optimistic estimate because the Haversine Distance between two points on Earth is the smallest distance between them. Roads are often not direct conduits between a start point and a destination. Hence, this heuristic is good.

We also normalise the heuristic to prevent it from overpowering the edge weights. This is once again done through min-max normalisation (Equation 2). Since both the travel time and glare components of the edge weights are normalized between 0 and 1, the edge weights are all values between 0 and 2. In order to keep the heuristic on the same scale as the edge weights, we multiply the normalized heuristic by 2 to scale it to the scale of the edge weights.

■ Results

Main Findings:

Table 1: A summary of the main findings in this investigation: aggregate glare, disengagement, and travel time improvement percent improvement values for statistically significant α - values in rural, suburban, and urban cities. An α -value of 0.1 meets all criteria for all types of cities.

City Type	α-value	Median Aggregate Glare Reduction (%)	Median Number of Disengagements Reduction (%)	Median Travel Time Increase for Aggregate Glare Experiment (%)	Median Travel Time Increase for Number of Disengagements Experiment (%)
Rural	0.1	8.6	0.0	1.8	1.1
	0.2	15.9	25.0	6.7	6.0
	0.3	18.7	16.7	11.9	10.9
	0.4	21.5	33.3	16.4	14.6
Suburban	0.1	23.9	25.0	6.0	5.8
	0.2	31.6	25.0	12.1	15.3
Urban	0.1	28.4	16.7	7.3	9.8
	0.2	36.0	Not Significant	15.4	Not Significant

As summarized in Table 1, the Sun-Aware Routing algorithm significantly reduced driver glare exposure across rural, suburban, and urban environments while maintaining travel times close to those of the benchmark shortest-path routes. For moderate glare-weighting values (α = 0.1–0.2), median aggregate glare decreased by approximately 9–36 %, with corresponding travel-time increases of only 2–15 %. These results indicated that modest adjustments to route cost weighting could yield substantial visibility and safety improvements.

When the model was applied to real-world Tesla Autopilot data, glare-related disengagements were concentrated at solar-cost values above 0.85, consistent with reduced visibility conditions. By avoiding these high-glare segments, the algorithm reduced predicted disengagement exposure by roughly 25–30 %, while maintaining efficient travel times. These findings, together with the statistical results in Table 1, provide preliminary evidence that incorporating real-time solar and atmospheric awareness into routing algorithms can enhance driving safety with minimal efficiency trade-offs.

Sun-Aware Routing Statistical Analysis

We evaluated 500 westward-facing paths for α ∈ [0, 1] at 7:50 PM in Fremont, a suburban city; San Francisco, an urban city; and Gilroy, a rural city on June 19, 2025, and report statistically significant results for any improvement in aggregate glare and travel time. We evaluate our model on these three development types to test its sensitivity to the setting.

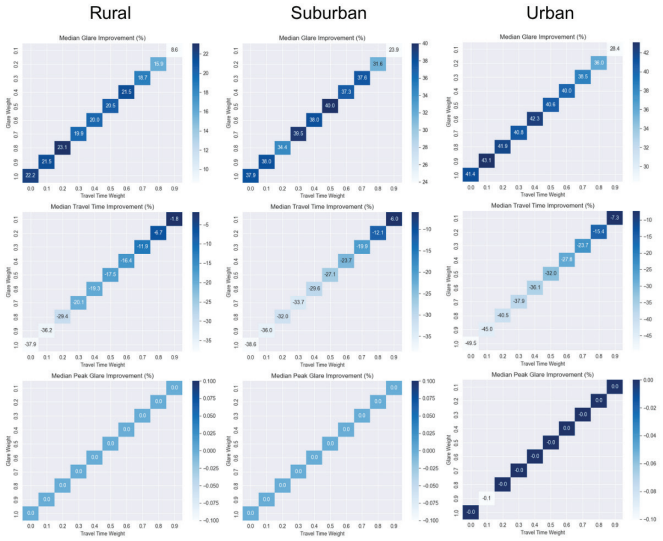

Figure 5: This figure compares the percentage changes in travel time and aggregate glare between the benchmark path and the sun-aware path for rural, suburban, and urban towns. Values of α from 0 to 1 in increments of 0.1 are evaluated. Certain α values result in significant glare reductions, as well as having travel time within a 20% increase of the benchmark.

From Figure 5, it is evident that increasing the glare-weight parameter (α) lowers both the mean and median aggregate glare, whereas raising the travel-time weight (1-α) lowers the mean and median extra travel time. In order to find the weights that result in an improvement in aggregate glare while keeping the travel time to within 20% of the benchmark value, we use a one-sided Wilcoxon signed rank test. Since the Wilcoxon tests are non-parametric, they do not require the assumption of normality of the differences.

The first test evaluated whether sun-aware routes reduced the aggregate glare metric, asking whether the median percent change in the aggregate glare between the calculated path and benchmark path was greater than zero. The second test evaluated whether the increase in travel time remained acceptable, testing whether the median percent change in travel time did not exceed 20%. Table 2 shows the p-values for each α-value across rural, suburban, and urban settings.

Table 2: Aggregate glare and travel time improvement p-values for different α in Gilroy (rural), Fremont (suburban), and San Francisco (urban). Bold entries indicate statistically significant results from the Wilcoxon Test. Bold and italicized α - values indicate those that satisfy the glare and travel time requirements for all geographic areas. α -values of 0.1 and 0.2 satisfy all the conditions.

α-value	Aggregate Glare (Rural)	Aggregate Glare (Suburban)	Aggregate Glare (Urban)	Travel Time Within 20% p-value (Rural)	Travel Time Within 20% p-value (Suburban)	Travel Time Within 20% p-value (Urban)
0.1	**< 0.001**	**< 0.001**	**< 0.001**	**< 0.001**	**< 0.001**	**<0.001**
0.2	**< 0.001**	**< 0.001**	**< 0.001**	**0.037**	**0.037**	**0.013**
0.3	**< 0.001**	**< 0.001**	**< 0.001**	**<0.001**	> 0.999	> 0.999
0.4	**< 0.001**	**< 0.001**	**< 0.001**	**0.035**	> 0.999	> 0.999
0.5	**< 0.001**	**< 0.001**	**< 0.001**	0.927	> 0.999	> 0.999
0.6	**< 0.001**	**< 0.001**	**< 0.001**	0.995	> 0.999	> 0.999
0.7	**< 0.001**	**< 0.001**	**< 0.001**	> 0.999	> 0.999	> 0.999
0.8	**< 0.001**	**< 0.001**	**< 0.001**	> 0.999	> 0.999	> 0.999
0.9	**< 0.001**	**< 0.001**	**< 0.001**	> 0.999	> 0.999	> 0.999
1.0	**< 0.001**	**< 0.001**	**< 0.001**	> 0.999	> 0.999	> 0.999

In the rural city of Gilroy (Table 2), the α -values of 0.1, 0.2, 0.3, and 0.4 all produce statistically significant decreases in aggregate glare while keeping the travel time to within a 20% increase of the benchmark. In the suburban city of Fremont and San Francisco (Table 2), the α -values of 0.1 and 0.2 are the only ones that lead to such results. Table 3 shows a summary of the results from the statistical analysis, and Figure 6 shows how the algorithm actively avoids high-glare paths by highlighting the divergence between the sun-aware route and the benchmark routes. In this particular instance, Fremont, a suburban city, was used with an α -value of 0.1.

Table 3: This table summarises the values that both decrease aggregate glare and keep the travel time within a 20% increase of the benchmark. α -values of 0.1 and 0.2 satisfy all the conditions.

City Type	α-value	Median Aggregate Glare Reduction (%)	Median Travel Time Increase (%)
Rural	0.1	8.6	1.8
	0.2	15.9	6.7
	0.3	18.7	11.9
	0.4	21.5	16.4
Suburban	0.1	23.9	6.0
	0.2	31.6	12.1
Urban	0.1	28.4	7.3
	0.2	36.0	15.4

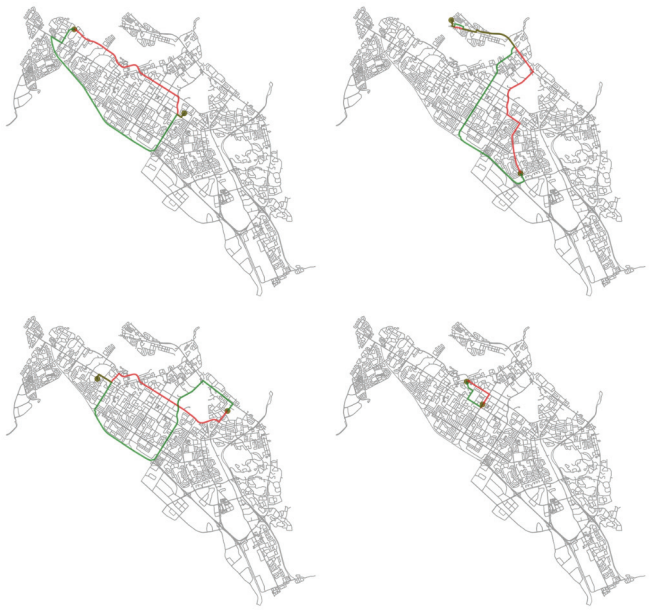

Figure 6: These maps illustrate the difference in route the sun-aware routing algorithm (green) takes compared to the shortest-length benchmark algorithm (red).

Autopilot Disengagement Mitigation

The subsequent part of our statistical analysis pertains to the prediction and mitigation of disengagements in 2021 Tesla Model Y cars during full self-driving. The results of this analysis are intended to be taken as preliminary results, as tests were conducted using only one vehicle, and minimal special measures were taken to control for external factors that may cause disengagements. The measures taken were the following: collecting data on a clear day, collecting data while on a main road in Fremont, California, and recording data as soon as the autopilot disengaged. The following is the data collected using the Compass app on an iPhone by taking a screenshot when the full self-drive disengages.

The following is the histogram of the frequency of each cost function value:

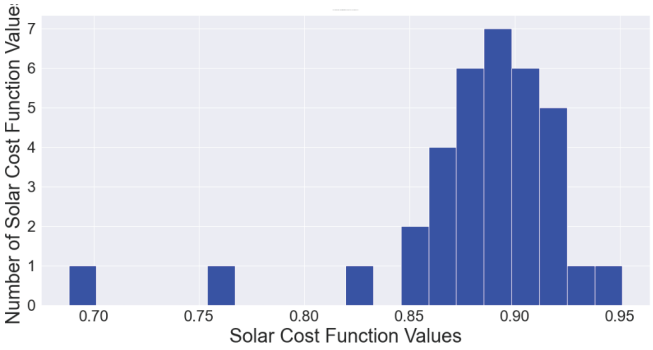

Figure 7: This figure shows the values of the solar cost function at which the full autopilot mode of the 2021 Tesla Model Y disengages due to poor visibility from glare. The distribution is fairly normal around the value 0.89.

We constructed a 99% confidence interval using the frequency data from Figure 7. Since this data is highly leftward skewed, we used Bootstrap resampling: (0.851, 0.899). We

DOI: 10.36838/IJHSR87.308

used the lower value, 0.851, as the cutoff for a 2021 Tesla Model Y being disengaged while on full autopilot.

Figure 8: This map illustrates the roads in Fremont, California, which have a solar cost function value greater than 0.851 at 7:50 PM on June 19, 2025. The roads facing northwest to southeast are the ones most affected by sun glare during this time.

We evaluated another 500 random westward-facing paths for $\alpha \in [0, 1]$ at 7:50 PM in Fremont, a suburban city; San Francisco, an urban city; and Gilroy, a rural city, on June 19, 2025, and report statistically significant results for any improvement in the number of 2021 Tesla Model Y disengagements and travel time. We measured a disengagement as a simple aggregate of the number of roads a commuter goes on, which has a sun glare weight of over 0.851. Figure 8 shows all such roads in Fremont, California, at 7:50 PM on June 19, 2025.

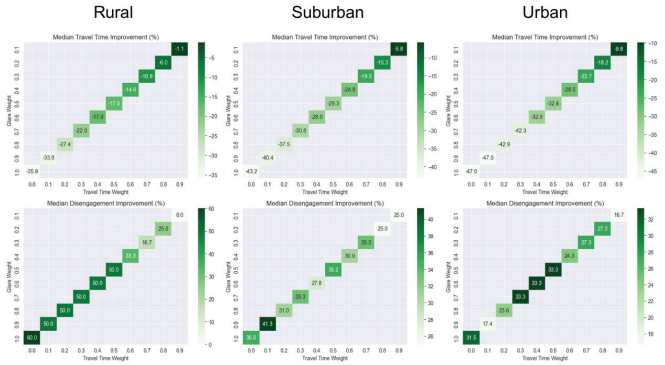

Figure 9: This figure compares the percentage changes in travel time and number of disengagements between the benchmark path and the sun-aware path for rural, suburban, and urban towns. Values of α from 0 to 1 in increments of 0.1 are evaluated.

Similarly to the previous grid-search, it is evident from Figure 9 that increasing the glare-weight parameter (α) lowers both the mean and median number of autopilot disengagements, whereas raising the travel-time weight (1-α) lowers the mean and median extra travel time. In order to find the weights that result in an improvement in the number of disengagements while keeping the travel time to within 20% of the benchmark value, we use two Wilcoxon signed rank tests again.

The first test evaluated whether sun-aware routes reduced the number of disengagements, asking whether the median percent change in the number of high-glare segments between the calculated path and benchmark path was greater than zero. The second test evaluated whether the increase in travel time remained acceptable, testing whether the median percent change in travel time did not exceed 20%. Table 4 shows the p-values for each α-value across rural, suburban, and urban settings.

Table 4: Number of disengagements and travel time improvement p-values for different α in Gilroy (rural), Fremont (suburban), and San Francisco (urban). Bold entries indicate statistically significant results from the Wilcoxon Test. Bold and italicized α -values indicate those that satisfy the disengagement and travel time requirements for all geographic areas. An α -value of 0.1 meets all criteria for all types of cities.

α-value	Disengagements (Rural)	Disengagements (Suburban)	Disengagements (Urban)	Travel Time (Rural)	Travel Time (Suburban)	Travel Time (Urban)
0.1	**< 0.001**	**< 0.001**	**< 0.001**	**< 0.001**	**< 0.001**	**< 0.001**
0.2	**< 0.001**	**< 0.001**	**< 0.001**	**< 0.001**	0.169	0.253
0.3	**< 0.001**	**< 0.001**	**< 0.001**	**< 0.001**	0.999	>0.999
0.4	**< 0.001**	**< 0.001**	0.220	**0.009**	> 0.999	> 0.999
0.5	**< 0.001**	**< 0.001**	**0.026**	0.789	> 0.999	> 0.999
0.6	**< 0.001**	**< 0.001**	**0.060**	0.992	> 0.999	> 0.999
0.7	**< 0.001**	**< 0.001**	**0.072**	> 0.999	> 0.999	> 0.999
0.8	**< 0.001**	**< 0.001**	0.3801	> 0.999	> 0.999	> 0.999
0.9	**< 0.001**	**< 0.001**	0.278	> 0.999	> 0.999	> 0.999
1.0	**< 0.001**	**< 0.001**	**0.035**	> 0.999	> 0.999	> 0.999

In the rural city of Gilroy (Table 4), the α-values of 0.1, 0.2, 0.3, and 0.4 all produce statistically significant decreases in the number of disengagements while keeping the travel time to within a 20% increase of the benchmark. In the suburban city of Fremont (Table 4), the α-values of 0.1 and 0.2 are the only ones that lead to such results. In the urban city of San Francisco (Table 4), only α = 0.1 produces statistically significant results. Table 5 shows a summary of the results from the statistical analysis.

Table 5: This table summarizes the values of α , which both decrease the number of disengagements and keep the travel time within a 20% increase of the benchmark. An α-value of 0.1 meets all criteria for all types of cities.

City Type	*α*-value	Median Number of Disengagements Reduction (%)	Median Travel Time Increase (%)
Rural	0.1	0.0	1.1
	0.2	25.0	6.0
	0.3	16.7	10.9
	0.4	33.3	14.6
Suburban	0.1	25.0	5.8
	0.2	25.0	15.3
Urban	0.1	16.7	9.8

Discussion & Limitations

The statistical analysis shows that a dynamic sun-aware routing algorithm can measurably reduce sun glare exposure without disproportionately increasing travel time. Despite these improvements, there still exist certain limitations to the algorithm. Firstly, the glare model does not currently incorporate roadside obstacles such as buildings, foliage, or overpasses, which could significantly alter glare. Secondly, the glare calculated on curved roads may be inaccurate due to the straight-road approximation, which was used while assigning weights to edges. Thirdly, these are pilot results gleaned from a sample size of one. Lastly, the evaluation algorithm ignores possible confounding variables like traffic conditions and other route differences. These issues are deferred to future work, which may include obstacle-aware glare, integration with high-resolution 3D map data, and a real-time traffic API.

The results confirm that for α-values of 0.1 and 0.2, the routing algorithm achieves statistically significant reductions in aggregate glare while keeping travel times within 20% of the benchmark path. In addition to improving glare metrics, the sun-aware algorithm shows potential for mitigating autonomous vehicle disengagements. Using disengagement data collected from a 2021 Tesla Model Y operating under full self-drive, we observed that glare-optimized routes reduced the number of high-glare roads (defined as edges in the graph with a glare function value exceeding 0.851) by up to 33.3% for $\alpha = 0.2$. These results indicate that glare-aware routing has direct applications in enhancing the safety and reliability of semi-autonomous vehicles that rely on camera-based feeds like the 2021 Tesla Model Y.

This work provides evidence that incorporating solar angle and atmospheric data into path planning can improve both human and autonomous navigation safety. The results demonstrate that glare-aware routing is a viable addition to existing navigation systems, particularly for commutes facing the sunrise and sunset.

Conclusion

This work introduces a sun-aware routing algorithm that integrates real-time solar position and atmospheric data into a modified A* search framework. By modeling glare as a function of solar geometry and cloud cover, we enable safer commutes, especially during sunrise and sunset. Across 500 westward test routes, our method reduced aggregate glare by a mean of 34.9% with only an 18.9% increase in travel time, and we identified a statistically significant optimal glare-weighting parameter ($\alpha = 0.1, 0.2$). These findings suggest that incorporating environmental context into routing can directly enhance driving safety.

Future work can improve the model's realism by incorporating 3D obstacle modeling using Google Street View data, as demonstrated in Guo *et al.*'s work. Dynamic traffic conditions could be integrated via APIs such as the TomTom Traffic API, while the weather model could be expanded to capture additional atmospheric effects, including the wavelength dependence of perceived glare. Evaluation could also be extended to a broader range of camera-based autonomous vehicles to better determine the glare-related disengagement threshold. Lastly, incorporating user-centered assessments of glare perception would provide a better understanding of safety and comfort impacts.

In terms of real-world adoption, this approach could be implemented as an optional routing feature in commercial navigation and autonomous driving systems, similar to existing options like "avoid highways" or "avoid tolls." Since these platforms already utilize real-time weather and satellite data, calculating solar position, cloud coverage, and glare intensity would require minimal additional infrastructure. This integration would make sun-aware pathfinding widely accessible, paving the way for safer and more context-aware navigation.

Acknowledgments

I would like to thank my mentor, Dr. Julia Milton, and the Indigo Research team.

References

1. S. Singh, "Critical reasons for crashes investigated in the National Motor Vehicle Crash Causation Survey," Traffic Safety Facts Crash Stats, Rep. DOT HS 812 506, Mar. 2018.
2. B. Bahnsen and Y. Mayster, "Navigation Suggestions to Select Driving Route with Low Sun Glare," 2022.
3. A. Das, N. R. Schneider, and H. Samet, "Safety-Aware Route Navigation: Driving with Less Sun Glare," in Proceedings of the 32nd ACM International Conference on Advances in Geographic Information Systems, in SIGSPATIAL '24. New York, NY, USA: Association for Computing Machinery, Nov. 2024, pp. 497–500. doi: 10.1145/3678717.3691225.
4. Y. Guo, J. Hu, R. Wang, S. Qu, L. Liu, and Z. Li, "Study on the influence of sun glare on driving safety," Building and Environment, vol. 228, p. 109902, Jan. 2023, doi: 10.1016/j.buildenv.2022.109902
5. X. Li, B. Y. Cai, W. Qiu, J. Zhao, and C. Ratti, "A novel method for predicting and mapping the presence of sun glare using Google Street View," Aug. 05, 2018, arXiv: arXiv:1808.04436. doi: 10.48550/arXiv.1808.04436.

Author

Rohin Vig is a high school student passionate about physics, computer science, research, and entrepreneurship. He enjoys applying computation to real-world problems and has led multiple independent research and entrepreneurship projects. Outside of academics, he builds educational tools and learns advanced topics in mathematics and physics.

DOI: 10.36838/IJHSR87.308